Cemil Çetinkaya[1], Ali Akay[2], Uğur Arabacı[1], Uğur Özdemir[1]*

[1] *Gazi University, Faculty of Technology, Metallurgical and Materials Engineering Department, 06560, Ankara, Turkey*
[2] *Birikim Engineering Co., 06909, Ankara, Turkey*

* *uozdemir@gazi.edu.tr*

EFFECT OF SHOP-PRIMER COATING ON S235JR STEEL ON MAG WELDABILITY

ABSTRACT

In this study, S235JR structural steel samples in uncoated condition and coated (shop-primer) in different thicknesses were welded by MAG (Metal Active Gas) welding method, and the effects of these applications on the mechanical and microstructure properties of the material were investigated. In the experimental studies, the first specimen group were used without any sandblasting and coating application, the second group specimens were sandblasted at Sa 2 ½ degree, and 25 µm, 50 µm, and 75 µm coatings were applied to the specimens in the other group. Surface conditions and coating thicknesses were selected as the variable parameters. With the examination of the radiography films, it was observed that the surface conditions affected the welded joint. As a result of the study, it was observed that altered coating thicknesses caused defects in the welding zone. It was determined that the coating thickness partially affected the mechanical properties, and the highest hardness values occurred in the weld zone in all samples. Relatively low values were obtained in tensile, bending and Charpy impact tests performed on sample groups with 75 µm coating thickness. The results were verified by the surface fracture, SEM, and EDS studies.

Keywords: Sandblasting, surface coating; shop-primer; MAG welding; microstructure

INTRODUCTION

Shop-primers are recommended to manufacturers by paint producers and are frequently used by manufacturers. Shop-primers are applied widely during the manufacturing of structural steels to increase corrosion resistance and to prepare for paint applications to be made in the next stages. In this study, the effects of shop-primers on weldability were investigated.

Paint producers stated that the purpose of applying the shop-primer is to protect structural components against corrosion during the manufacturing phase with structural steels and storage and manufacturing before the first paint system is applied. The film thickness of a shop-primer should normally be 20 - 25 µm. This thickness is specified for smooth test panels. Steel materials and structural parts coated with shop primer can be welded [1-3]. In some cases, when the surface coating is improper in terms of indecency of chemical

composition or excessive coating thickness, welding process can cause porosity [4-5]. Berendsen reported that the conditions requiring the application of shop primer would form the basis for the final paint system by providing adequate protection against corrosion during shipbuilding or offshore manufacturing [6]. In the study of portable welding robots by Blasko et al., shop primed (20 ± 2 μm thickness) welds were analyzed. It has been noted that slower welding speeds and oscillating motion are required when welding shop-primed materials with the robot. They stated that unless the material required more than three weld layers, interpass cleaning would not be necessary [8]. Solic et al. reported that the shop primer coating did not have a negative effect on the quality of the welded joints in their studies [9]. Zhabrev et al. examined the effect of coatings in 10 different compositions on the welding process and quality, and stated that all coatings used in the study, including shop-primer coating, had a negative effect on bead-on-plate welding stability [7]. Chung et al. investigated post-weld corrosion resistance and porosity formations by applying different shop-primer products at different drying times and at different thicknesses [4]. According to the porosity formation formation obtained from the collected data, it was observed that the porosity decreased as the drying time of the coating decreased, and the porosity increased as the coating thickness increased. Ahsan et al., on the other hand, mentioned the pores formed in the weld due to heat input in the GMAW welding study of cold metal transfer zinc-coated steel [10].

In this study, the effects of shop primer on MAG weldability will be revealed by experimental studies. As a result of the experimental study, the effects of shop primer coating will be scientifically investigated and the results will be evaluated.

MATERIALS AND METHOD

In this study, S235JR structural steels, which are widely preferred in industrial production, were used. The chemical composition and mechanical properties of the samples are given in Table 1. The sample sizes used for experimental studies were determined as 4x150x350 mm. Some of the samples were used as a produced condition, and the others were sandblasted as Sa 2 ½ according to TS EN ISO 8501-1 to avoid any foreign matter on the surface of the materials and to increase the adhesion of the paint to the surface before shop primer coating at different thicknesses was applied (Table 2). After these applications, the samples were joined by the MAG welding method. After these procedures, visual inspection, macrostructure, microstructure and radiography tests, and mechanical tests (hardness, tensile, bending, and notch impact test) were applied to all samples.

Table 1. Chemical composition (% wt) and mechanical properties of S235JR material

C	Mn	P	S	Cu	Al	Cr	Ti
0.09	0.53	0.018	0.011	0.008	0.037	0.025	0.002

Yield Strength (MPa)			Tensile Strength (MPa)			Elongation (%)	
	285			388			40

Table 2. Sample naming and surface treatment status

No	Sample code	Sample condition	Applied shop primer thickness
1	M1	As Produced	-
2	M2	Sandblasting	-
3	M3	Sandblasting + shop primer	25 μm ± 5 μm
4	M4	Sandblasting + shop primer	50 μm ± 5 μm
5	M5	Sandblasting + shop primer	75 μm ± 5 μm

After sandblasting, shop primer was applied to the samples. Shop primers are two-component epoxy polyamides containing zinc phosphate pigments used as rust inhibitors. The general properties of the shop primer used in the experimental studies are given below, and the chemical content of the shop primer is given in Table 3.

- Color tone   : Red
- Solids by % volume   :26 ± 1
- Flash point   : 4 °C
- Hard Drying   : 6 min., 20°C
- Application method   : Airless spray / Air spray / Brush (touch-up)
- Thinner (max. by Volume) : % 20
- Dry film thickness   : 20 μm ± 5 μm

Table 3. Typical chemical composition of shop primer coating (% wt.)

H	P	Ca	Mg	Al	Cr	Zn	Si	O	C
5.8	1.5	5	3.3	0.2	0.8	3.8	3.2	35.6	43.8

Welding wire and its properties used with MAG robotic welding machine for all samples, including shop primer coated ones, are given in Table 4, and welding parameters and properties that are kept constant during the test during the welding processes are given in Table 5.

Table 4. Properties of the welding wire used in the study

Classification			
TS EN ISO 14341-A	G42 3CM G3Si1		
AWS A5.18	ER70S-6		
Chemical Analysis (% wt.) – (Typical)			
C	Si		Mn
0.08	0.85		1.50
Mechanical properties of weld metal (Typical)			
Yield Strength (N/mm^2)	Tensile Strength (N/mm^2)	Elongation (%)	Impact Resistance (J)
440	540	30	60 (-30 ^{0}C)

Table 5. Welding parameters and consumable properties

Welding Current (A)	Arc Voltage (V)	Wire Feed Speed (cm/min.)	Comm. Name	Wire Diameter (mm)	Flow Rate of Shielding Gas (L/min)	Heat Input (kJ/mm)
215-220	22	44	SG2	1.2	19	5.2
Shielding Gas:		$M24 : Ar + CO_2\ 12\% + O_2\ 2\%$				

RESULTS AND DISCUSSIONS

In this section, the results of the effects of surface preparation and shop primer coating thickness on all test specimens are evaluated. First of all, visual inspections were made on the samples according to the acceptance criteria specified in the TS EN ISO 5817 standard. Cap and root seam photos of S235JR structural steel after robotic MAG welding are given in Figure 1.
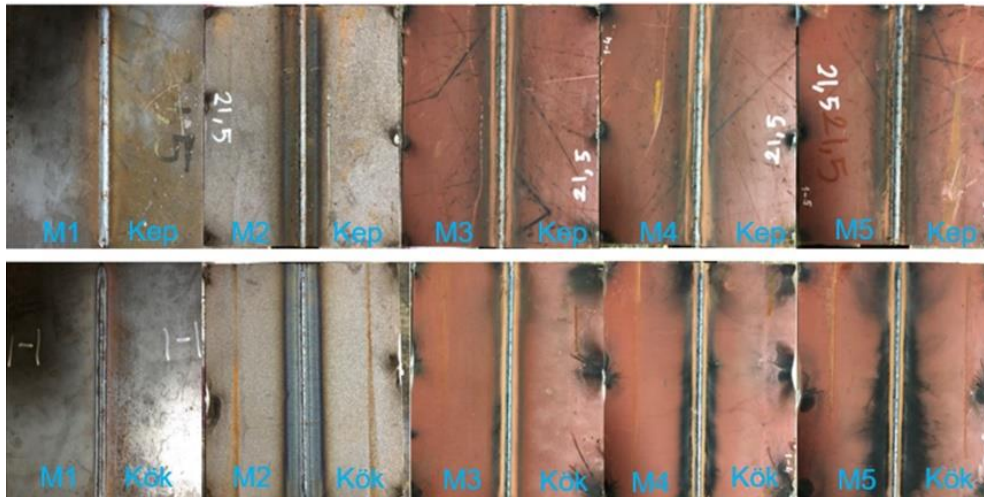
Fig. 1. Cap and root photos of S235JR structural steel after robotic MAG welding

The visual inspection control process was carried out by a specialist qualified following the TS EN ISO 9712 standard and by us, in an environment that fulfills the requirements for the standards to be applied. In the observation made during the welding of M3, M4, and M5 samples, it was observed that the amount of smoke emitted from the welding increased as the coating thickness increased. In addition, in the evaluation made on the back surfaces of the painted materials after welding, it was observed that the blackening in the sample increased as the paint thickness increased.

In the macro examinations made after the samples welded with the robotic MAG method in Figure 2, it was seen that the height did not exceed the maximum 3 mm value given for excessive penetration in the TS EN ISO 5817 standard 504.
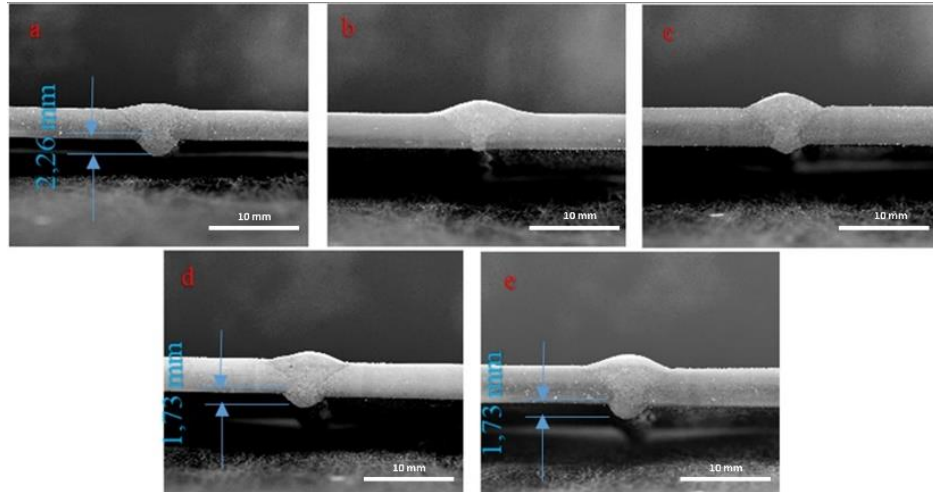
Fig. 2. Macrographs of welded samples by robotic MAG welding method a) M1, b) M2, c) M3, d) M4, and e) M5 samples

The highest value measured in the M1 sample was 2.26 mm, which is within the acceptance criteria. As a result of the macro examination, no melting defect, lack of penetration, pore, crack, and residue was detected in the samples. In the test of the structural properties of MAG welding of S235JR materials by Solic et al., it has been shown that there are no visible defects and deviations in the macro photographs in the weld region between the samples covered with a protective coating and the reference samples [9].

In the microstructure analysis, grain structure, welding heat inputs, and phase transformations as a result of cooling were determined. The main material microstructure photograph of S235JR structural steel is given in Figure 3.
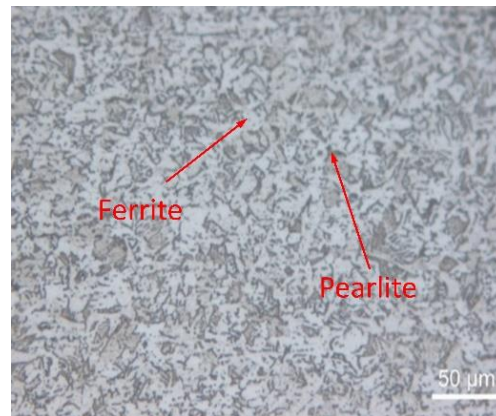

Fig. 3. Base metal microstructure photograph of S235JR structural steel

When the microstructure photograph of the base material of S235JR structural steel in Figures 4-8 is examined, the regions in black represent pearlite and the regions in light color represent ferrite. Due to the low carbon content, it is seen that the pearlite phase ratio is low, and the ferrite phase ratio is higher.

In Figures 4-8, the microstructure photographs of the weld metal, melting point, and coarse-grained regions of all samples are given. Then these results were evaluated together.
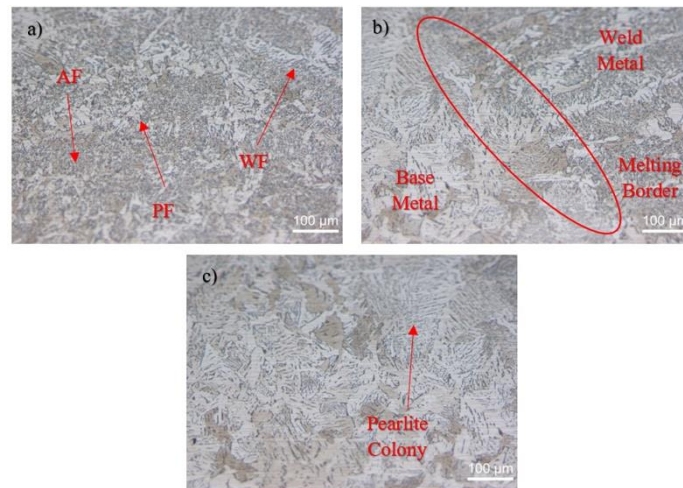
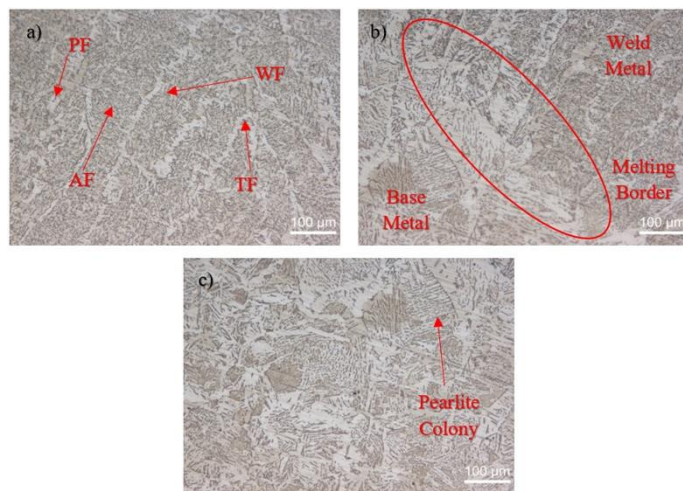**Fig. 4.** Weld zone micrographs of M1 sample, a) weld metal, b) transition zone, c) coarse-grained zone

Fig. 5. Weld zone micrographs of M2 sample, a) weld metal, b) transition zone, c) coarse-grained zone
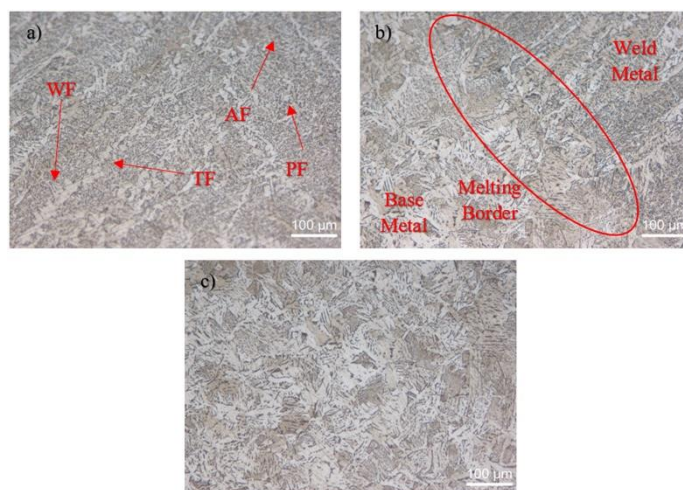

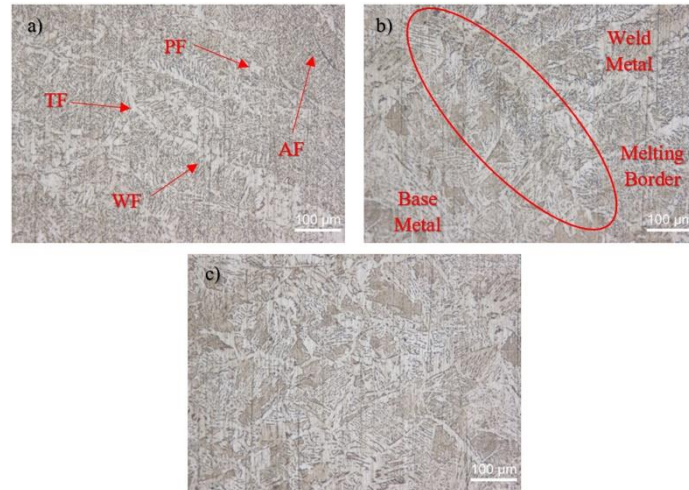**Fig. 6.** Weld zone micrographs of M3 sample, a) weld metal, b) transition zone, c) coarse-grained zone

Fig. 7. Weld zone micrographs of M4 sample, a) weld metal, b) transition zone, c) coarse-grained zone
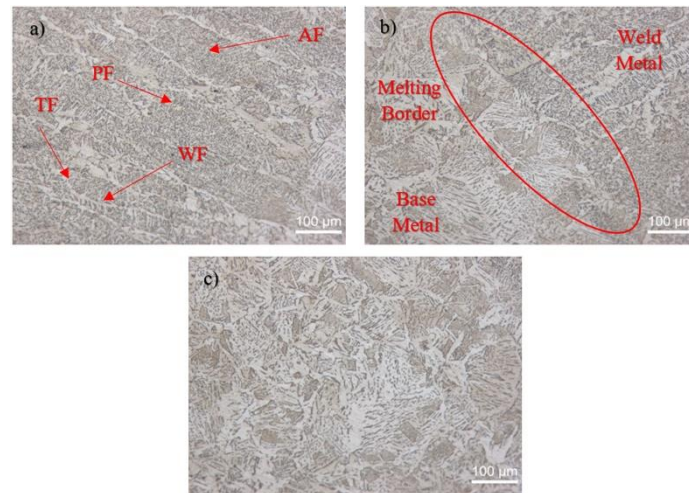

Fig. 8. Weld zone micrographs of M5 sample, a) weld metal, b) transition zone, c) coarse-grained zone

In the microstructure examination of the samples at X100 magnification, the weld metal shows characteristic features. Depending on the heating and cooling in the heat-affected region, a change in the internal structure compared to the weld metal was detected. The microstructure of the M group weld metal is markedly different from that of the base metal of similar composition, as shown in the pictures. The difference in microstructure is related to the different thermal histories of the base metal and weld metals, not the chemical composition. Acicular (AF), widmanstatten (WF), grain boundary (TF), and polygonal ferrite (PF) structures were determined in the weld metal microstructures of M group samples welded by the MAG method. According to the literature, it has been reported that similar structures are obtained in welded joints of low carbon steels [11,12]. As a result of microstructural studies, no significant difference was observed on the samples that were combined with the same parameters on the materials with and without fabrication pre-primed by MAG welding. The effects of the coating thickness were not observed in the microstructure examinations of the welded joints made by changing the shop primer coating thickness of 25, 50, and 75 µm on the M3, M4, and M5 samples.

In Figure 9, radiography films of the welding regions of M group samples joined with robotic MAG welding are given.
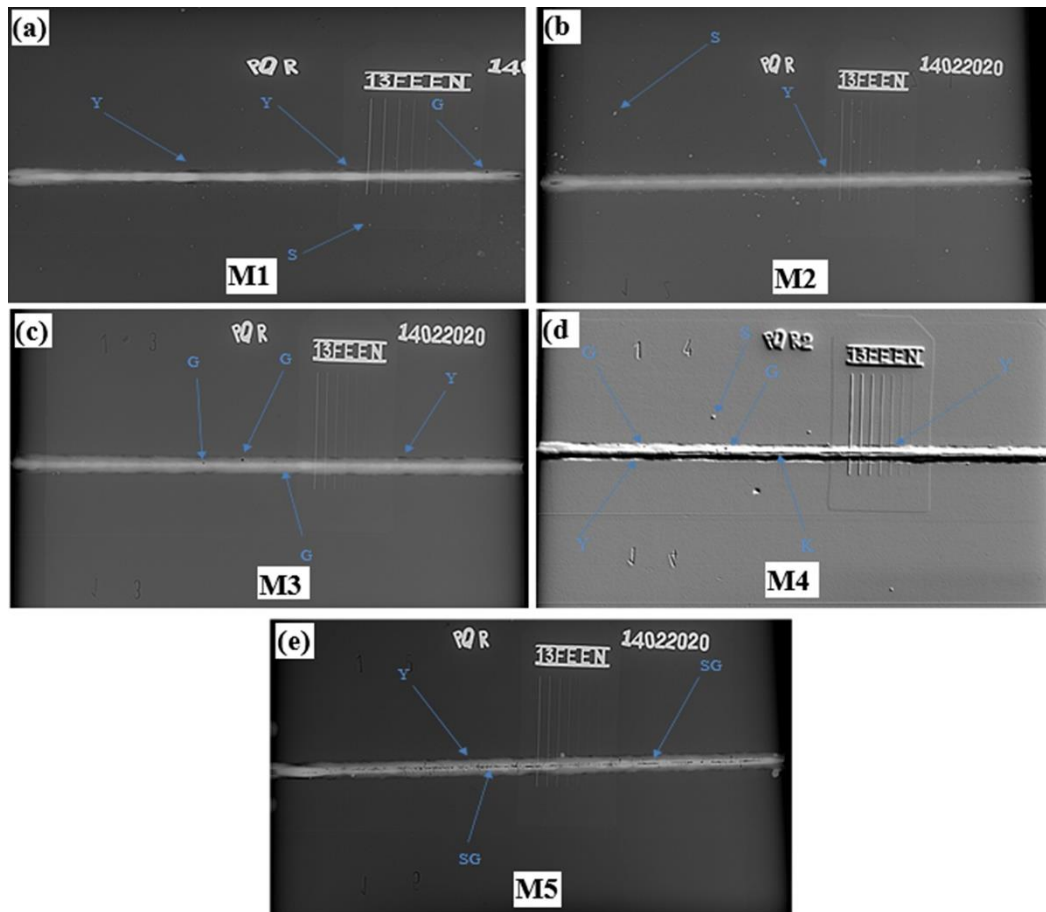
Fig. 9. Radiographic photographs of welded samples joined by MAG welding method a) M1, b) M2, c) M3, d) M4 and e) M5

In Figure 9, Y represents combustion grooves, G pores, S spatters, K deficiencies, and SG rows of pores. As a result of the radiographic examination of M1, M2, M3, and M4 samples, burning grooves, excessive penetration, and pore formation defects that may occur in robotic MAG welding were detected, and the detected defects were accepted within the standards. In the study of Akay et al., as a result of radiographic examination, the inadequacy of penetration that may occur in the weld, burning grooves, pore formation, residues, cracks, etc. defects were observed, and the observed were accepted within the norms, they explained [13]. It was observed that the pores detected in M3, M4, and M5 samples were caused by the applied zinc-based shop primer application. Ahsan et al., in their study, explained the pore formation, growth and escape behavior, and mechanical properties of weld joints in CMT-GMAW over a wide heat input range (150-550 J/mm). However, pore formation, growth, and escape mechanisms have been described in the literature using the viscosity of the weld pool and the vapor pressure of the zinc [10,14,15]. Although defects were detected in the M3 and M4 samples with shop primer coating, the pores and sequential pores below the maximum 3 mm specified in the TS EN ISO 10675-1 acceptance criteria were included in the acceptance criteria.

Figure 10 shows the points where the hardness measurements are taken on the weld metal cross-section. Here (0) represents the weld metal, (1) and (-1) ITAB, (2) and (-2) the base material.
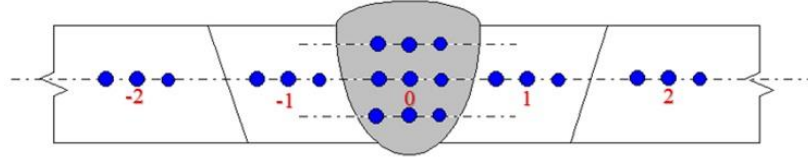
Fig. 10. Points where hardness measurements were taken on the weld metal section

In Figure 11, the hardness results of M group samples welded by the robotic MAG welding method are given.
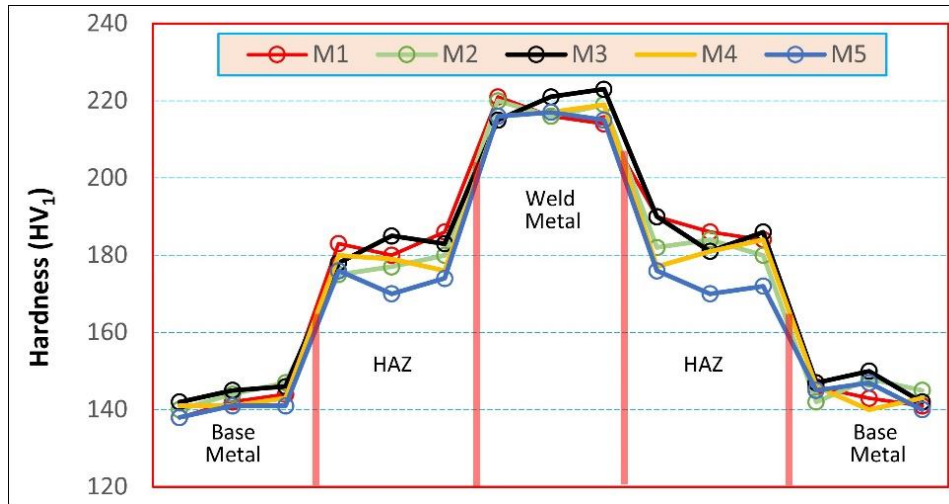

**Fig. 11**. Hardness graph of M group samples

In the hardness graph of the M group samples given in Figure 2, it is seen that the highest hardness occurs in the weld metal. It is thought that one reason for this increase in hardness in the weld metal is the Mn contribution of the additional wire used, and the other reason is the microstructures formed by thermal transformation. Başyiğit and Solak, in their study of the effect of S235 structural steel on the mechanical and microstructural properties, explained the reason for this as the carbon content of the welding wire supporting the total carbon amounts in the weld metal regions. In this way, the hardenability of the weld metal region is preserved compared to the heat-affected regions under the cooling conditions of the welding processes [16]. In the examinations made on the M group samples, it was seen that sandblasting, and the manufacturing front primer of different thicknesses used within the scope of the study did not have any effect on the hardness. Because the coating, which is rich in zinc, could not penetrate the weld metal due to burning and fragmentation due to the high temperatures during welding, it did not have any effect that would affect the hardness.

The tensile test results of all M group samples welded with robotic MAG welding are given in Table 6.

Table 6. Tensile results of samples welded with MAG welding

Sample Code	Number of Samples	Tensile Test Speed (mm/min.)	Tensile Strength Avg. (MPa)	Cross-sectional Narrowing Avg. (%)	Elongation Avg. (%)
M1	3	15	402	55	25
M2	3	15	403	58	24
M3	3	15	401	56	24
M4	3	15	402	57	24
M5	3	15	400	57	23

Figure 12 shows SEM images taken from the fractured surfaces of M specimens after the tensile test.
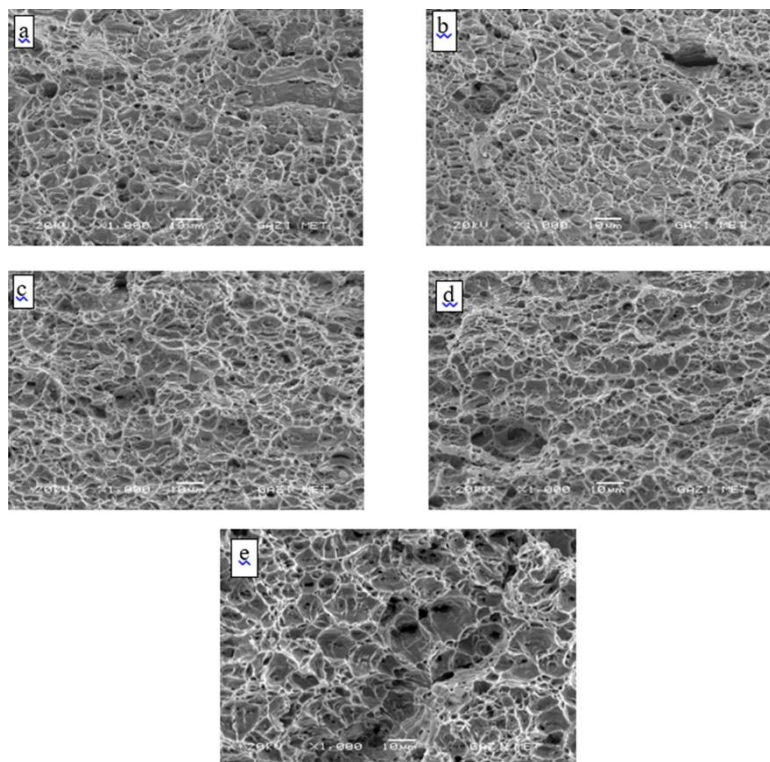
Fig. 12. SEM images of the fracture surfaces of specimens. a) M1, b) M2, c) M3, d) M4 and e) M5

In the tensile test, all samples ruptured in the base metal, outside the weld metal, and the HAZ region. It was observed that the tensile strength of the welded samples was slightly higher than the tensile strength of the base metal. The reason for this is that the strength of the HAZ and the weld metal has increased due to the welding process, and it has been seen that more force is needed to perform the deformation in these regions. As the ductile part in the tensile region narrowed, it caused a slight increase in tensile strength. In the study of Kahraman et al., it showed higher strength because the welded region prevents deformation during the tensile test. Since the tensile samples are prepared by the standards, the deformation occurs outside of this region due to the hardness of the weld zone in the welded samples. The fact that the deformation occurred in a narrow region also caused high strength [17]. When the fracture surfaces formed as a result of tensile were examined, the appearance of the fracture surfaces showed that the S235JR steel was subjected to ductile fracture with fibrous structures and honeycomb appearance due to its structure and low carbon content. As

shown in various previous studies, the fracture can occur due to void coalescence or mechanical instability of the sample itself. First, cavities nucleate in inclusions and then grow with the help of plasticity. As the enlarged spaces coalesce, a crack forms, and the material breaks. The ductile fracture of the S235JR sample subjected to plastic deformation has been described in the literature [18-22]. Depending on the chosen method, sandblasting and increased shop primer coating thickness in the samples welded with robotic MAG did not affect the results of the tensile test although they affected the welding quality. However, it is thought that the sequential pores seen on the M5 sample are on the cap side of the weld and were removed from the surface during the preparation of the samples by the tensile sample processing method.

In Figure 13, the notch impact test results of M group samples joined with robotic MAG welding are given graphically.
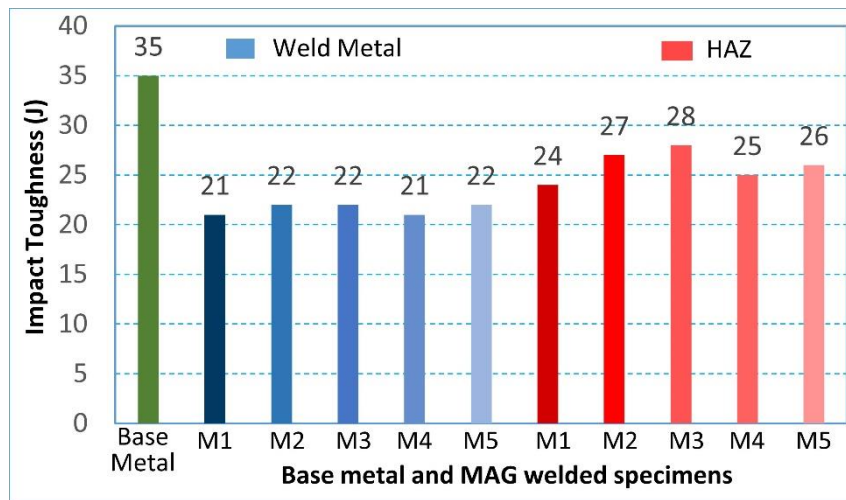

Fig. 13. Notch impact results of M group samples

Since the thickness of the welded material is 4 mm and the notch standard is 10 mm, the notch impact samples made with non-standard test dimensions (55x10x4 mm.) were tested at room temperature. The notch impact toughness of S235JR steel was measured as 35 J and the toughness of the welding wire used was given as 60 J. For the M group samples obtained as a result of the experiment, the values were measured as 21 J, 22 J, 22 J, 21 J, 22 J in the weld metal, and as 24 J, 27 J, 28 J, 25 J, and 26 J in the HAZ, respectively. The notch impact values obtained as a result of the experiments were obtained in the highest base material, then in the HAZ, and then in the weld metal, respectively. Increasing hardness due to the additional metal used in the weld metal and cooling rates decreased the toughness. In HAZ, on the other hand, increasing hardness due to grain coarsening and cooling rate occurs at higher values than the weld metal, reducing the impact energy absorption power, and lower results were obtained than the base material. In the study of Durgutlu et al., the main material showed the highest notch impact strength, followed by HAZ and weld metal, respectively [23]. Çetinkaya reports in a study that the toughness decreases as the hardness increases. Likewise, the notch impact strengths obtained from the weld metal were found to be lower than the values obtained from HAZ [23]. In a study on the fracture behavior of HAZ in welding low carbon steels, it was stated that the toughness of the coarse-grained zone in HAZ

was higher than that of the weld metal. In addition, the hardness of HAZ is lower than the weld metal hardness, which confirms this result [24].

The purpose of root and cap surface bending tests on butt welded M group test specimens is to evaluate the ductility or weld discontinuities at or near the surface of the joint. The test results for this purpose are determined as a cap and root bending test sample, as can be seen in Figure 14, and prepared following the TS EN ISO 5173 standard and subjected to the bending test.
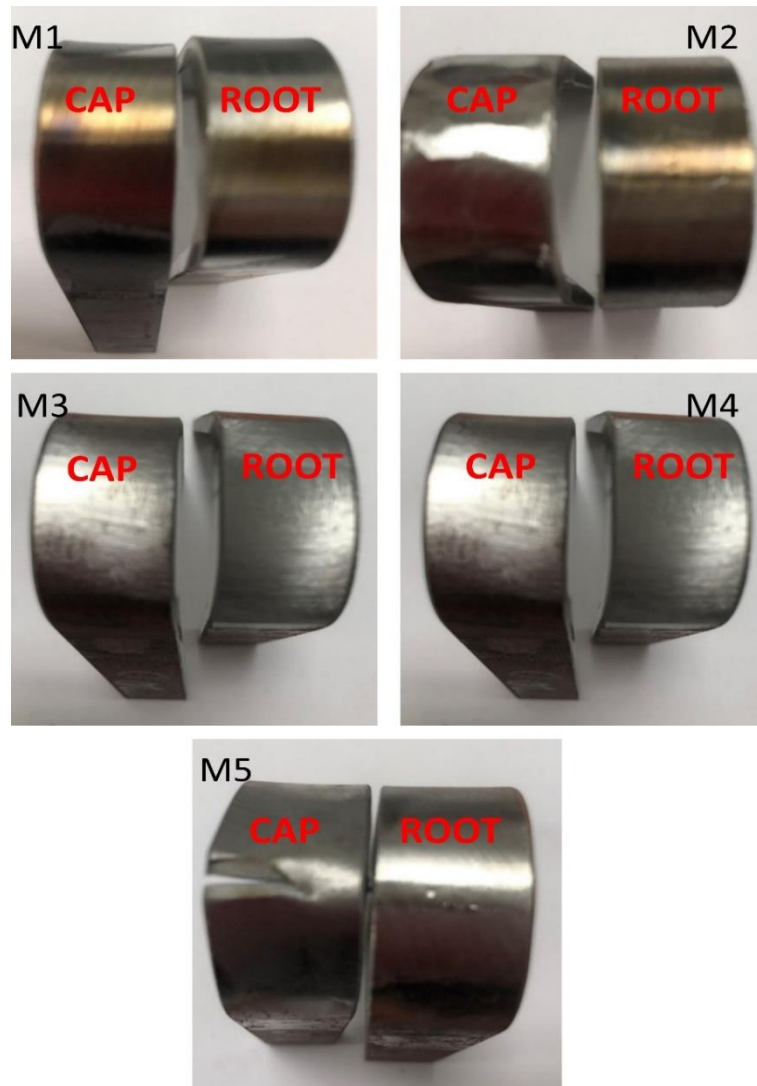

Fig. 14. Bending test results of M group samples

When Figure 16 is examined, no cracks are observed in the welded joint area after the cap and root bending test performed on M1, M2, M3, and M4 samples. The formability of the welded material is good, and this shows that the joint fulfills the formability conditions, and the hardness of the weld zone of the material used does not reach the hardness that can be broken by bending. In the literature review, considering that the crack state is directly proportional to the amount of elongation in the bending test, it can be concluded that the amount of elastic transformation allows for a U-type bending ratio. This shows that the weld

metal exhibits bending strength as much as the base material. Therefore, weld metal is suitable for use in the field as base materials [25-27]. In the bending tests of M1, M2, M3, and M4 specimens joined by the robotic MAG welding method, no cracks that would affect the formability of the welded joint were detected. Sandblasting of the material as supplied and coating thickness of 25 µm and 50 µm did not have any adverse effect on the bending test. However, a crack was detected in the M5 sample with 75 µm shop primer applied. In the evaluation made after the bending test for the M5 specimen, no cracks were detected in the root region, but cracks were observed in the cap part. It is thought that the pores seen in the radiography film affect this crack formation.

CONCLUSIONS

In this study, 4 mm thick S235JR quality materials were welded to M2, M3, M4, and M5 samples by MAG method after surface treatment, and to M1 sample without surface treatment.

- In the samples joined by the robotic MAG welding method, the amount of burning and darkening in the coating increases depending on the coating thickness. Depending on the coating thickness, the amount of smoke output increased during welding. It has been observed that arc initiation becomes more difficult as the coating thickness increases. It was observed that the arc started in the material that was sandblasted the easiest and then in the material that did not undergo any treatment.
- When the microstructure photographs were examined, it was observed that similar microstructures were formed in the samples welded with robotic MAG. Widmanstaten ferrite, acicular ferrite, and polygonal ferrite microstructure are observed in the weld metal. In this internal structure formation, soft ferrite sheets and hard perlite colonies are intertwined, so the region where this structure is formed becomes harder and more brittle than the base metal. The reason for the formation of this structure is the high cooling rate. Different coating thicknesses and surface preparation had no effect on the microstructure.
- When the results of the radiographic examination were examined, it was seen that the M2 sample was within the standards, and there was no welding defect. The reason for this is the removal of rust and rolling wastes that will affect the welding ability on the surface by sandblasting. It was determined that porosity (porosity) occurred in M1, M3, M4, and M5 samples. The porosity formed in the M1 sample was caused by the rolling scraps and the wastes on the surface. It is considered that the porosity formed in M3, M4, and M5 samples is within the scope of acceptance criteria and is due to the trapping of the shop primer coating applied in the weld pool during welding.
- According to the hardness results, it was observed that the hardness values of the whole sample increased gradually from the base material to the weld metal. There was no correlation between hardness results and surface treatments and increased coating thickness.
- It was found that tensile tests broke from the main material in all samples except for the weld area, and their mechanical values were higher than the standard requirement of at least 360 MPa. Ductile fracture properties were observed in the rupture surface SEM examinations, the surface condition and coating thickness had no effect on the samples.

- In all samples, as a result of notch impact tests, the toughness values of the weld metal were found to be lower than the HAZ and base material toughness values.
- Bending tests were successful in all samples except the M5 sample, and it was seen that the welds obtained were suitable for formability. As a result of the 180° bidirectional bending tests of all samples except the M5 sample, no visible defects were detected. The damage seen in the M5 sample showed that the coating thickness had a negative effect on the formability of the weld.

REFERENCES

1. Hempel: Doğru boya sistemi nasıl seçilmeli. Korozyona karşı koruyucu boyalar için ISO 12944 standardına uygun temel esaslar ve sistemler. Hempel Coatings, İstanbul, 2017, pp. 14-16.

2. JOTUN: Coating Manual, Jotun Paints, Sandefjord, 1999, 3(5) - 15.37.

3. Teknos: Handbook, For Corrosion Protection of Steel Surfaces by Painting, (Second Edition), Teknos Oy, Finland, 2013, pp. 9-65.

4. Chung, S., Hyun, J.: Methodological approach of evaluation on prefabrication primers for steel structures, International Journal of Naval Architecture and Ocean Engineering, 13, (2021) 707-717.

5. D'Addona D.M., Genna S., Giordano A., Leone C., Matarazzo D., Nele L.: Laser Ablation of Primer During the Welding Process of Iron Plate for Shipbuilding Industry, Procedia CIRP, 33, (2015) 464-469.

6. Berendsen M.: Marine Painting Manual, Springer, Netherlands, 1989, pp. 167-169.

7. Zhabrev, L., Kurushkin, D., Mushnikov, I., Panchenko, O.: The Coatings Breakdown Products Influence on the Gas Metal Arc Welding Parameters, Coatings, 10, (2020) 1061.

8. Blasko G.J., Moniak D.J., Howser B.C.: Evaluation of hitachi zosen portable welding robotics, 92' Ship Production Symposium Proceedings, Welding Panel, U.S. Navy: News Shipbuilding, 1992, 8A-1.

9. Solic T., Maric D., Jagodic Z., Samardzic I.: Testing Of The Shopprimer's Influenceon The Quality Of Welded Joint. Metalurgıja, 56, 3-4 (2017) 357-360.

10. Ahsan M.R., Kim Y.R., Ashiri R., Cho Y.J., Jeong C., Park Y.D.: Cold Metal Transfer (CMT) GMAW of Zinc-Coated Steel. Welding Journal, 95 (2016) 120-132.

11. Parmar, R.S.: Welding Engineering And Technology, (First Edition), Khanna Publisher, Delhi, 1995, 659-700.

12. Fydrych, D., Łabanowski, J., Rogalski, G., Haras, J., Tomków, J., Świerczyńska, A., Jakóbczak, P., Kostro, Ł.: Weldability of S500MC Steel in Underwater Conditions, Advances in Materials Science, 14, 2, (2014) 37-45.

13. Akay, A.A., Kaya, Y. ve Kahraman, N.: Tozaltı Ark Kaynak Yöntemi ile Birleştirilen X60, X65 ve X70 Çeliklerin Kaynak Bölgesinin Etüdü. Karaelmas Fen ve Mühendislik Dergisi, 3, (2013) 34-42.

14. Carestream: NDT Images An Overview, Your guide to proper processing and interpretation of radiography films for Non-Destructive Testing (NDT), Carestream, Inc., New York, 2000.

15. IAEA: Introduction to Radiographic Examination, Nondestructive Examination (NDE) Technology and Codes, Student Manual, 1, 5.0, IAEA Technical Training Center, Vienna, 2008.

16. Başyiğit A.B., Solak B.: The Effects of Flux Type on Mechanical and Microstructural Properties of S235 Structural Steel by Submerged Arc Welding, El-Cezerî Fen ve Mühendislik Dergisi, 7(2), (2020) 659-666.

17. Kahraman N., Gülenç B. and Durgutlu A.: Tozaltı Ark Kaynağı İle Kaynaklanan Düşük Karbonlu Çeliklerde Serbest Tel Uzunluğunun Mikroyapı ve Mekanik Özelliklere Etkisinin Araştırılması. G.Ü. Fen Bil. Ens Dergisi, 18(3), (2005), pp. 473-480.

18. Bahman A.R. and Alialhosseini E.: Change in hardness, yield strength and UTS of welded joints produced in St37 grade steel, Indian Journal of Science and Technology, 3-12 (2010) 1162-1164.

19. Kossakowski P.G.: Experimental Determination Of The Void Volume Fraction For S235JR Steel At Failure In The Range of High Stress Triaxialities, Arch. Metall. Mater., (2017) 167-172.

20. Pineau A., Benzerga A.A., Pardoen T.: Failure of metals I: Brittle and ductile fracture, Acta Materialia 107 (2016) 424-483.

21. Aşıkuzun, E., Çetinkaya, C., Boz, M., Ada, H.: Fracture Surface Investigations of Api Pipes Welded With Parameters Determined By Taguchi Method. Sakarya University Journal of Science, 22-5 (2018) 1392-1402.

22. Biner İ.: Kaynaklı Numunelerin Tahribatlı Testlerinin Güvenilirliği ve Cihaz Kalibrasyonu, Kaynak Kongresi IX. Ulusal Kongre ve Sergisi, Ankara, Turkey, 2015, pp. 125-129.

23. Çetinkaya C.: Düşük karbonlu çeliklerin tozaltı ark kaynak yöntemi ile kaynak edilebilirliği ve mekanik özelliklerinin incelenmesi. Gazi Üniversitesi Fen Bilimleri Enstitüsü Dergisi, 12-2 (1999) 279-293.

24. Apay S. and Demirbaş U.: S355J2+N Malzemelerin Elektrocuruf Kaynak Yöntemi ile Kaynaklanabilirliği ve Mekanik Özeliklerinin İncelenmesi. Düzce University Journal of Science and Technology, 8-1 (2020) 940-950.

25. Kobelco: Weld Imperfections and Preventive Measures, Kobe Steel Ltd, Tokyo, Japan, 2015, pp. 1-19.

26. Guo J., Xu X., Jepson M.A., Thomson R.C.: Influence of weld thermal cycle and post weld heat treatment on the microstructure of MarBN steel. International Journal of Pressure Vessels and Piping, 174 (2019) 13-24.

27. Çiçek B, İş E.G., Gümüş E. and Topuz P.: The Effect of Welding Positions on the Weldability of X20CrMoV11-1 Steels. Hittite Journal of Science and Engineering, 5-1 (2018) 75-83.